Published in final edited form as:
J Immunol. 2010 January 1; 184(1): 173–183. doi:10.4049/jimmunol.0902372.

ATP-Binding Cassette Transporter G1 Negatively Regulates Thymocyte and Peripheral Lymphocyte Proliferation

Allison J. Armstrong[*,†], **Abraham K. Gebre**[‡], **John S. Parks**[‡], and **Catherine C. Hedrick**[†,§,¶]

[*]Department of Pharmacology, University of Virginia, Charlottesville, VA 22908

[†]The Robert M. Berne Cardiovascular Research Center, University of Virginia, Charlottesville, VA 22908

[¶]Department of Molecular Physiology and Biological Physics, University of Virginia, Charlottesville, VA 22908

[‡]Department of Pathology/Lipid Sciences, Wake Forest University School of Medicine, Winston-Salem, NC 27157

[§]La Jolla Institute for Allergy and Immunology, La Jolla, CA 92037

Abstract

Cholesterol is a key component of cell membranes and is essential for cell growth and proliferation. How the accumulation of cellular cholesterol affects lymphocyte development and function is not well understood. We demonstrate that ATP-binding cassette transporter G1 (ABCG1) regulates cholesterol homeostasis in thymocytes and peripheral CD4 T cells. Our work is the first to describe a cell type in Abcg1-deficient mice with such a robust change in cholesterol content and the expression of cholesterol metabolism genes. Abcg1-deficient mice display increased thymocyte cellularity and enhanced proliferation of thymocytes and peripheral T lymphocytes in vivo. The absence of ABCG1 in CD4 T cells results in hyperproliferation in vitro, but only when cells are stimulated through the TCR. We hypothesize that cholesterol accumulation in *Abcg1*$^{-/-}$ T cells alters the plasma membrane structure, resulting in enhanced TCR signaling for proliferation. Supporting this idea, we demonstrate that B6 T cells pretreated with soluble cholesterol have a significant increase in proliferation. Cholesterol accumulation in *Abcg1*$^{-/-}$ CD4 T cells results in enhanced basal phosphorylation levels of ZAP70 and ERK1/2. Furthermore, inhibition of ERK phosphorylation in TCR-stimulated *Abcg1*$^{-/-}$ T cells rescues the hyperproliferative phenotype. We describe a novel mechanism by which cholesterol can alter signaling from the plasma membrane to affect downstream signaling pathways and proliferation. These results implicate ABCG1 as an important negative regulator of lymphocyte proliferation through the maintenance of cellular cholesterol homeostasis.

Lymphocytes undergo rapid proliferation during development in the thymus and in response to antigenic challenge. The least mature double-negative (DN) CD4^{-} CD8^{-} thymocytes can be divided into four subsets (DN1–4) using the expression of two markers, CD25 and CD44: CD25^{-}CD44^{+} (DN1), CD25^{+}CD44^{+} (DN2), CD25^{+}CD44^{-} (DN3), and CD25^{-} CD44^{-} (DN4). DN4 cells give rise to double-positive (DP) CD4^{+} CD8^{+} cells, which mature into

Address correspondence and reprint requests to Dr. Catherine C. Hedrick, La Jolla Institute for Allergy and Immunology, Division of Inflammation Biology, 9420 Athena Circle, La Jolla, CA 92037. hedrick@liai.org .

Disclosures The authors have no financial conflicts of interest.

The online version of this article contains supplemental material.

$CD4^+$ or $CD8^+$ single-positive (SP) cells (1). The first cell expansion occurs during the DN1 to DN3 stages before TCRβ gene rearrangement; the second occurs during the DN–DP transition before TCRα gene rearrangement. During this process, thymocytes receive stage-specific growth signals from autonomous cells and the thymic microenvironment. Pre–TCRβ-induced proliferation (DN1–DN3) is dependent on c-kit and IL-7 signals provided by epithelial cells (1, 2). Late DN3, DN4, and DP proliferation signals are derived from the pre-TCR complex and trigger a maturation program within developing thymocytes that includes rescue from apoptosis, inhibition of further DNA recombination at the TCRβ gene, and induction of proliferation and differentiation (3).

After T cell selection and maturation occurs in the thymus, naive T cells enter the periphery and circulate to secondary lymphoid organs awaiting an encounter with Ag (4). Complex homeostatic mechanisms assure the survival and production of lymphocytes in appropriate numbers to maintain proper immune cell function. Evidence suggests that TCR interaction with self-MHC is necessary for survival and expansion of peripheral T cells (5). The TCR signal delivered in the periphery maintains the homeostasis of the naive T cell pool by keeping cells alive and alert. Further, the low level of proliferation reaffirms the potential of the T cell to respond to infection and launch a full immune response.

Following TCR ligation, a cascade of signaling events occurs that ultimately results in the induction of IL-2 gene expression, cell-cycle entry, proliferation, and T cell effector functions (6). Signals from the thymocyte pre-TCR involve many of the same signaling proteins and lead to survival, differentiation, proliferation, and allelic exclusion (1). Ligation of the TCR also induces rapid lipid raft clustering that results in the concentration of TCR signaling proteins at the area of contact between APCs and T cells, known as the immunological synapse (7). Lipid rafts are highly ordered cholesterol and ganglioside–rich platforms that facilitate and coordinate close interactions between signaling molecules to amplify downstream signaling. Patients with autoimmune diseases, such as systemic lupus erythematosus, have hyperactive T cells with a lower TCR activation threshold. Further, systemic lupus erythematosus T cells have increased plasma membrane cholesterol and lipid raft formation, suggesting that changes in cholesterol plasma membrane levels can enhance protein–protein interactions and TCR signaling (8).

Cholesterol is a key component of cell membranes and is essential for cell growth and proliferation (9). Cholesterol homeostasis is maintained by two main nuclear receptor systems: sterol regulatory element binding proteins (SREBPs) and liver X receptors (LXRs). SREBP-2 resides in the endoplasmic reticulum under conditions of ample sterol (10). When low cholesterol levels are sensed, SREBP-2 is cleaved and transported into the nucleus to activate genes involved in cholesterol synthesis and uptake, such as low-density lipoprotein receptor (LDLR), 3-hydroxy-3-methylglutaryl-CoA (HMG-CoA) reductase and HMG-CoA synthase (10). Alternatively, under conditions of excess cellular cholesterol, the LXR pathway is induced, which increases cholesterol efflux through the lipid transporters ATP-binding cassette A1 (ABCA1) and ATP-binding cassette transporter G1 (ABCG1) (11). Recently, Bensinger et al. (12) demonstrated that proliferating T cells maintain cholesterol homeostasis although the reciprocal regulation of SREBP and LXR. Cells only proliferate if enough cholesterol is available to satisfy this metabolic checkpoint.

Although the function of ABCG1 has been described as a lipid transporter, very little is known about how ABCG1 facilitates the removal of cholesterol. ABCG1 is localized in intracellular compartmental membranes and has been shown to mobilize to the plasma membrane upon cholesterol loading of macrophages (13), although the study by Xie et al. (14) does not support this finding. Tarr and Edwards (15) showed that ABCG1 is localized to intracellular vesicles in primary mouse hippocampal neurons and primary mouse

astrocytes. The importance of ABCG1 and how it maintains cholesterol homeostasis in other cell types is not clear. ABCG1 plays a critical role in maintaining lipid homeostasis in a variety of organs and is highly expressed in the ileum, liver, lung, spleen, and kidney (16, 17). *Abcg1*$^{-/-}$ mice accumulate lipid in their liver and lungs but not in the spleen, kidney, or ileum when fed a high-fat/high-cholesterol diet (18). At 6 mo of age, *Abcg1*$^{-/-}$ mice on chow diet display cellular accumulation, macrophage and pneumocyte type 2 cell hypertrophy, increased levels of surfactant, and massive lipid accumulation (19). We and other investigators showed that lipid accumulation in *Abcg1*$^{-/-}$ lungs begins at a very early age and is accompanied by massive inflammatory cell recruitment and cytokine production (20, 21). Further, a bone marrow–derived cell is responsible for pulmonary lipidosis and inflammation in *Abcg1*$^{-/-}$ mice (20). ABCA1 expression is not able to compensate for the loss of ABCG1 in the lung or immune cells, probably because of differences in the way ABCA1 and ABCG1 maintain cholesterol homeostasis. ABCA1 effluxes cholesterol to lipid-poor ApoA1, whereas ABCG1 promotes cholesterol efflux to more mature high-density lipoprotein particles (22, 23). Because ABCG1 expression is primarily intracellular, and *Abcg1*$^{-/-}$ cells have no impairment of cholesterol efflux, the primary role of ABCG1 might be to regulate subcellular cholesterol distribution.

How cholesterol homeostasis affects lymphocyte development and function is not well understood. In this study, we found that the absence of ABCG1 resulted in a quantitative increase in cholesterol content and hyperproliferative thymocytes and peripheral lymphocytes. Our data demonstrate that cholesterol content in the membrane is very important to TCR signaling, and the absence of ABCG1 resulted in increased ZAP70 and ERK1/2 phosphorylation. Inhibiting ERK1/2 phosphorylation in *Abcg1*$^{-/-}$ T cells rescued the hyperproliferative phenotype. We can now use *Abcg1*$^{-/-}$ mice as a model to investigate how disruptions in intracellular cholesterol homeostasis affect lymphocyte development and function. We demonstrate an unrecognized mechanism of how increased cholesterol content can regulate TCR signaling and cellular proliferation, which could severely impact the immune response.

Materials and Methods

Reagents

Flow cytometry Abs anti-mouse CD4 (L3T4), TCRβ (H57–597), CD69 ([^{1}H].2F3), CD25 (PC61.5), CD3ε (17A2), CD62L (MEL-14), CD45.1 (A20), and CD45.2 (104) were purchased from eBioscience; CD8 (53-6.7) and CD44 (IM7) were purchased from BD Pharmingen (San Diego, CA), and lineage marker mixture, TCRαβ and CD4 was purchased from Caltag Laboratories (Burlingame, CA). CFSE, PMA, ionomycin, and soluble cholesterol were purchased from Sigma-Aldrich (St. Louis, MO). Murine recombinant IL-2, anti-mouse CD3, and anti-mouse CD28 were purchased from BD Pharmingen. Thymidine methyl ^{3}H was purchased from PerkinElmer (Wellesley, MA). PD98059 was purchased from BIOMOL (Plymouth Meeting, PA). Dynabeads T activator CD3/CD28 were purchased from Invitrogen (Carlsbad, CA).

Mice

C57BL/6 (stock no. 000664) and B6.129S7-RAG1$^{tm1Mom/J}$ (stock no. 002216) mice were purchased from The Jackson Laboratory (Bar Harbor, ME), *Abcg1*$^{-/-}$/lacZ knock-in mice on a C57BL/6J background were purchased from Deltagen (San Mateo, CA), and B6.SJL-Ptprca/BoyAiTac mice were purchased from Taconic Farms (Germantown, NY). Mice were fed a standard rodent chow diet and housed in microisolator cages in a pathogen-free facility. All experiments followed University of Virginia Animal Care and Use Committee guidelines, and approval for use of rodents was obtained from the University of Virginia.

Purification of naive CD4 T cells and in vitro proliferation assays

Spleen was excised and pushed through a 70-μm strainer. Total CD4 T cells or naive CD4 T cells ($CD4^+CD62L^+$) were purified using Miltenyi Biotec (Auburn, CA) isolation kits and the manufacturer's protocol. For CFSE-dilution experiments, cells were stained with CFSE dye at 5 μm for 5 min and washed extensively. Purified cells were plated at 5×10^4 cells/well in a 96-well U-bottomed plate coated with αCD3 Ab. Soluble αCD28 was added at a concentration of 1 μg/ml. For ^{3}H-thymidine–incorporation experiments, ^{3}H-thymidine was added 48 h after seeding, and incorporation was measured 16–18 h later. In some experiments, 10 μM PD98059 was added to cultures when cells were plated. For cholesterol-loading experiments, T cells were preincubated with 20 μg/ml cholesterol-loaded methyl-β-cyclodextrin for 2 h before stimulation with αCD3αCD28 beads.

Flow cytometry

One to four $\times 10^6$ cells were resuspended in 100 μl staining buffer (1% BSA, 0.1% sodium azide in PBS). Cells were blocked with Fcγ receptor for 10 min and stained with flow cytometry Abs for 30 min at 4°C. A fixable LIVE/DEAD stain (Invitrogen) was used for viability. Cells were fixed with 2% paraformaldehyde. Samples were run on a CyAn ADP LX 9 Color analyzer (DakoCytomation), and data analyses were performed with FlowJo software (Tree Star, Ashland, OR). Cells were gated on forward versus side scatter then viability dye. The absolute numbers were calculated by multiplying the percentage of cells in individual subsets by the total cell count before staining. To visualize lipid rafts, splenocytes were first labeled with CD3 and CD4, as described above, and then rapidly stained with 10 ng Alexa Fluor 488–labeled cholera toxin B (CT-B) from Vybrant lipid raft–labeling kits (Invitrogen) for 10 min at 4°C. Cell fluorescence was determined using a FACSCalibur flow cytometer (BD Biosciences, San Jose, CA) and analyzed with FlowJo software (version 7.2.2). The mean fluorescence intensity was quantified, and the expression relative to B6 was calculated.

Cholesterol content in T cells

Three $\times 10^6$ T cells were pelleted by low-spin centrifugation. After several washes with PBS, the cell pellet was extracted with isopropanol containing 5-cholestane as internal standard. Total and free cholesterol content was determined by gas–liquid chromatography and normalized to cellular protein, as previously described (24). Cholesteryl ester was calculated as (total cholesterol 2 free cholesterol) × 1.67. Multiplying by 1.67 corrects for the average fatty acid mass that is lost during saponification.

Quantitative real-time PCR

Total cellular RNA was collected from T cells using a Qiagen RNeasy Kit (Valencia, CA) following the manufacturer's protocol. One microgram of cDNA was synthesized using an Iscript cDNA synthesis kit (Bio-Rad, Hercules, CA). Total cDNA was diluted 1:8 in H_2O, and 2 μl were used for each real-time condition using a Bio-Rad MyIQ single-color real-time PCR detection system and iQ SYBR Green supermix (Bio-Rad). Primer sequences are listed in Supplementary Table I. Data were analyzed and presented on the basis of the relative expression method (25). The formula for this calculation is as follows: relative expression = $2^{-(S\Delta C_t - C\Delta C_t)}$ where ΔC_t is the difference in the threshold cycle between the gene of interest and the housekeeping gene (18S), S is the *Abcg1*$^{-/-}$ mouse, and C is the C57BL/6J control mouse.

In vivo proliferation studies

For homeostatic proliferation experiments, naive CD4 T cells were purified from B6 and *Abcg1*$^{-/-}$ mice and labeled with CFSE. Two $\times 10^6$ cells/genotype were coinjected into the

tail vein of *RAG*$^{-/-}$ mice. After 7 d, the spleens were harvested and stained for CD4, CD69, CD25, CD3, CD45.1, CD45.2, and LIVE/DEAD dye for viability. For in vivo BrdU incorporation experiments, mice were given an i.p. injection of 1 mg BrdU in 100 μl. Thymus and spleen were harvested after 4 h, and BrdU incorporation was detected by following the manufacturer's protocol in the APC BrdU Flow Kit (BD Pharmingen, cat 51-9000019BK). Thymocytes were stained with a lineage marker mixture, CD44, CD4, CD25, CD3, CD8, and LIVE/DEAD viability dye. Splenocytes were stained with CD3, CD4, CD8, and LIVE/DEAD viability dye.

Short-term in vitro T cell stimulation and Western blots

Three to five × 10^6 purified naive CD4 T cells were incubated with 20 μg/ml αCD3 and αCD28 on ice for 30 min. After washing, Abs were crosslinked with goat anti-hamster IgG at 37°C. Cells were lysed in radio immuno precipitation assay buffer, separated by SDS-PAGE, and immunoblotted with the indicated Abs. Anti-ZAP70, anti–phospho-ZAP70 (Tyr319), anti-PLCγ1, anti–phospho-PLCγ1, anti–phospho-JNK1/2, anti-JNK1/2, and anti-p38 were purchased from Cell Signaling Technology (Beverly, MA). Anti–phospho-ERK1/2 and anti–phospho-p38 were purchased from R&D Systems (Minneapolis, MN). Anti-ERK1/2 and anti–β-actin were purchased from Santa Cruz Biotechnology (Santa Cruz, CA).

Statistical analysis

Data for all experiments were analyzed using Prism software (GraphPad, San Diego, CA). The EC_{50} for thymidine incorporation experiments was calculated using nonlinear regression curve fit. Unpaired *t* tests and two-way ANOVA were used to compare experimental groups. Data are graphically represented as mean ± SEM. A p value <0.05 was considered significant.

Results

ABCG1 regulates thymocyte development and peripheral T cell proliferation in vivo

To investigate the role of ABCG1 in lymphocyte development and peripheral proliferation, we examined the thymus and spleen of 5- to 8-wk-old *Abcg1*$^{-/-}$ mice on a C57BL/6 background. We observed no visual difference in gross morphology of the spleen or difference in the total cellularity or weight of spleens from C57BL/6 (B6) and *Abcg1*$^{-/-}$ mice (Fig. 1A–C). Flow cytometry analysis revealed no change in the frequency of CD4 versus CD8 T cells (Fig. 1D) at 6–8 wk of age. However, at 5 wk of age, *Abcg1*$^{-/-}$ mice had a visibly larger thymus (Fig. 2A) and a 60% increase in the total thymic cellularity (Table I), implicating that global loss of ABCG1 alters T lymphocyte development. We observed only slight differences in the frequencies of DP, DN, and SP populations in *Abcg1*$^{-/-}$ mice, specifically, a small increase in the percentage of DP ($CD4^+CD8^+$) thymocytes with a concomitant decrease in the percentages of the DN ($CD4^-CD8^-$) and CD8 SP populations and no significant change in the percentages of the CD4 SP population (Fig. 2B). However, when comparing total cellularity of these populations, we found an ~50% increase in the number of DP, DN, and CD4 SP cells in Abcg1−/− mice and no change in the number of CD8 SP cells (Table I). The ratio of DN/DP thymocytes in *Abcg1*$^{-/-}$ mice (1:25.0 ± 0.8) was significantly higher than in B6 mice (1:20.6 ± 0.3; $p < 0.0001$). This suggested an increase in the proliferation that occurs during the DN to DP transition. We further investigated the DN thymocyte subpopulations to determine whether ABCG1 expression altered the transition and proliferation of these subsets. Flow cytometry analysis of the DN subpopulations revealed a slight decrease in the DN4 thymocyte subset in *Abcg1*$^{-/-}$ mice (Fig. 2C). We hypothesize that the *Abcg1*$^{-/-}$ thymocytes are more proliferative and have an accelerated DN4 to DP transition, which provides an explanation for the decrease in the frequency of DN4 thymocytes and the increase in DP thymocytes.

A dynamic increase in the total number of thymocytes hinted that enhanced thymocyte proliferation occurs in the absence of ABCG1. We investigated thymocyte and peripheral T cell proliferation in vivo by measuring BrdU incorporation. Although the spleen from *Abcg1*$^{-/-}$ mice appeared normal (Fig. 1A), we observed a 37% increase in CD4^{+} and a 77% increase in CD8^{+} T cell homeostatic proliferation in *Abcg1*$^{-/-}$ mice compared with B6 mice (Fig. 3A, 3B). This low level of proliferation occurs through MHC–TCR engagement, suggesting that the absence of ABCG1 in T cells results in increased MHC–TCR interactions or stronger signals from the TCR. When we examined BrdU incorporation in the thymus, we observed a 20% increase in DN2 proliferating thymocytes, a 10% increase in DN3 proliferating thymocytes, and a 27% increase in DP proliferating thymocytes (Fig. 3C, 3D). These findings suggest that the increased thymic cellularity in *Abcg1*$^{-/-}$ mice (Table I) is probably due to the hyperproliferation of developing thymocytes.

ABCG1 regulates cholesterol content in lymphocytes

Modulating cholesterol levels can alter membrane structure and signaling from the TCR (26), but very little is known about basal cholesterol levels in lymphocytes. We measured cholesterol content using gas chromatography in resting B6 and *Abcg1*$^{-/-}$ CD4 T cells purified from the spleen. Surprisingly, we found a 3.4-fold increase in cholesteryl ester accumulation in *Abcg1*$^{-/-}$ T cells (Fig. 4A). This is the first cell type in Abcg1-deficient mice to be described with such a robust change in cholesterol content, and little is known about the ability of the T cell to accumulate cholesterol (18, 27–29). Moreover, we found a dramatic decrease in mRNA expression of proteins involved in cholesterol synthesis and uptake. *Abcg1*$^{-/-}$ CD4 T cells had a 74% reduction in SREBP-2, a 91% reduction in LDLR, a 67% reduction in HMG-CoA reductase, and a 66% reduction in the expression of HMG-CoA synthase (Fig. 4B), consistent with endoplasmic reticulum cholesterol loading, as elegantly shown by Radhakrishnan et al. (30). We also measured LXR target genes and observed a 6.4-fold increase in ABCA1 and a 2.2-fold increase in SREBP-1c expression in *Abcg1*$^{-/-}$ resting CD4 T cells compared with B6 T cells (Fig. 4B). These data provide evidence that LXR transcriptional activity is increased in *Abcg1*$^{-/-}$ T cells. Cholesterol is an important component of membrane lipid rafts, and lipid raft perturbations were shown to modulate TCR signaling (26). Therefore, we quantified the membrane lipid raft content in B6 and *Abcg1*$^{-/-}$ CD4 T cells using fluorescently labeled CT-B, which binds to the pentasaccharide chain of ganglioside GM1, a raft-associated lipid. We observed a 38% increase in lipid raft in the plasma membrane of resting *Abcg1*$^{-/-}$ CD4 T cells, as measured by higher CT-B staining intensity (Fig. 4C). We expect that proteins involved in TCR signaling may be clustered within the rafts of resting *Abcg1*$^{-/-}$ T cells, making them “primed” for proliferation.

Given our results so far, we hypothesize that cholesterol accumulation in *Abcg1*$^{-/-}$ T cells causes the hyperproliferative phenotype. We were interested in determining whether loading B6 T cells with cholesterol would enhance their proliferative capacity. We measured the proliferation of B6 and *Abcg1*$^{-/-}$ naive CD4 T cells that were pretreated with soluble cholesterol before TCR stimulation. Remarkably, we observed a 30% increase in thymidine incorporation by B6 T cells loaded with cholesterol (Fig. 4D), suggesting that cholesterol availability can drive T cell proliferation. Conversely, cholesterol loading did not affect the proliferation of *Abcg1*$^{-/-}$ T cells (Fig. 4D). Perhaps the beneficial effects of excess cholesterol in *Abcg1*$^{-/-}$ T cells have been maximized and the addition of cholesterol confers no more advantage under these conditions.

Finally, because we found increased proliferation by thymocytes and peripheral lymphocytes, we wanted to determine whether ABCG1 also regulated cholesterol homeostasis in the thymus. Similar to peripheral T cells, we found a 15–20% decrease in the mRNA expression of SREBP-2, LDLR, and HMG-CoA reductase in *Abcg1*$^{-/-}$ thymocytes

(Fig. 4E), suggesting increased cholesterol content in *Abcg1*$^{-/-}$ thymocytes as well. Moreover, we found a 45% increase in ABCA1 expression (Fig. 4E), further confirming a disruption in cholesterol homeostasis in the thymocytes. The changes in thymocyte expression levels of cholesterol metabolism genes were not as dramatic as peripheral CD4 T cells. We believe this is because thymocytes are rapidly proliferating and constantly using cholesterol for membrane formation. However, peripheral T cells proliferate slowly under homeostatic conditions and, therefore, have the opportunity to accumulate cholesterol. This finding gives us a model to investigate how excess cholesterol can affect T cell function and TCR signaling.

Abcg1$^{-/-}$ CD4 T cells are hyperproliferative

Our results demonstrated that thymocytes and peripheral T cells in *Abcg1*$^{-/-}$ mice are hyperproliferative and have impaired cholesterol homeostasis. To definitively determine whether *Abcg1*$^{-/-}$ naive CD4 T cells have a proliferative advantage in vivo, we used a competitive adoptive transfer model of homeostatic proliferation. In this model, proliferation is controlled by TCR–MHC interactions in the lymphopenic environment (4). Naive CD4^{+} T cells were purified from B6 (CD45.1^{+}) and *Abcg1*$^{-/-}$ (CD45.2^{+}) mice, labeled with CFSE, and coinjected into *Rag*$^{-/-}$ mice. After 7 d, splenocytes were analyzed for proliferating T cells by gating on CD4^{+} cells, because a subset of proliferating T cells had downregulated CD3 expression. Remarkably, we observed a 6-fold increase in the frequency of *Abcg1*$^{-/-}$ CD4 T cells compared with B6 T cells (Fig. 5A,5B). When we evaluated CFSE profiles of B6 versus *Abcg1*$^{-/-}$ CD4 T cells, we found that the majority (>99%) of *Abcg1*$^{-/-}$ T cells were CFSE^{low}, whereas 25% of B6 T cells remained CFSE^{high} (Fig. 5C). These data clearly demonstrate that the absence of ABCG1 provides naive CD4 T cells with a homeostatic proliferative advantage.

Subsequently, we investigated the proliferation of *Abcg1*$^{-/-}$ CD4 T cells in vitro. Naive CD4 T cells were purified from the spleens of B6 and *Abcg1*$^{-/-}$ mice and stimulated with plate-bound αCD3 in the presence or absence of costimulatory soluble αCD28. We found that TCR stimulation with αCD3 alone resulted in a 2.4-fold increase in ^{3}H-thymidine incorporation; the addition of costimulatory αCD28 resulted in a 2.2-fold increase in ^{3}H-thymidine incorporation in *Abcg1*$^{-/-}$ T cells (Fig. 6A). Flow cytometry analysis of CFSE dilution revealed that the *Abcg1*$^{-/-}$ T cells divided more frequently compared with B6 CD4 T cells (Fig. 6B). Furthermore, cell cycle analysis revealed that *Abcg1*$^{-/-}$ T cells had an increase in the percentage of cells in the S, G_2, or M phase (Fig. 6C) after 48 h of stimulation. These in vitro data re-capitulate what was observed in vivo and suggests that after TCR stimulation, *Abcg1*$^{-/-}$ T cells progress more quickly through the cell cycle.

Next, we wanted to investigate the mechanism by which *Abcg1*$^{-/-}$ T cells are hyperproliferative. Because IL-2 is an essential cytokine for proliferation, we examined whether ABCG1 expression impacted IL-2 production and signaling. We found no increase in the amount of IL-2 produced by *Abcg1*$^{-/-}$ CD4 T cells, measured by IL-2 mRNA expression and IL-2 protein levels in the supernatant of proliferating cultures (data not shown). Additionally, excess IL-2 added to the proliferating cultures did not abrogate the difference in proliferative capacity of the *Abcg1*$^{-/-}$ T cells (Fig. 6A). We also measured CD25 and CD69 expression after stimulation (24 and 48 h) to determine whether ABCG1 expression impacts lymphocyte activation; we found no significant difference in the upregulation of these activation markers (data not shown). These data strongly suggest that T cell activation and IL-2 signaling are not the mechanisms by which *Abcg1*$^{-/-}$ CD4 T cells are hyperproliferative. An alternative hypothesis was that the absence of ABCG1 resulted in a “survival” advantage culminating in decreased apoptosis and increased proliferating cells. We measured cell surface Annexin V levels after 24 and 96 h of stimulation in vitro and found no difference in cell viability or Annexin V^{+} cells between B6 and *Abcg1*$^{-/-}$ T cells

(data not shown). Our data imply that the regulation of proliferation by ABCG1 is not attained through alterations in IL-2 signaling, lymphocyte activation, or a survival advantage.

Because we found that the absence of ABCG1 results in increased cholesterol accumulation and lipid raft formation in CD4 T cells, we hypothesized that modulation of lipid rafts and/or membrane cholesterol would alter TCR signaling. We first considered the possibility that *Abcg1*$^{-/-}$ T cells had a lower TCR threshold. To investigate this hypothesis, we stimulated B6 and *Abcg1*$^{-/-}$ naive CD4 T cells with increasing concentrations of plate-bound αCD3 and soluble αCD28. We found that *Abcg1*$^{-/-}$ T cells had a similar sensitivity to TCR stimulation compared with B6 T cells (Fig. 6D), with no significant difference in the EC_{50} values for proliferation of B6 and *Abcg1*$^{-/-}$ CD4 T cells (EC_{50} B6 $10^{2.60 \pm 0.32}$; *Abcg1*$^{-/-}$ $10^{2.78 \pm 0.38}$). Therefore, we concluded that TCR sensitivity is not the primary mechanism by which *Abcg1*$^{-/-}$ T cells are hyperproliferative.

Subsequently, we wanted to determine whether signals from the TCR are necessary for *Abcg1*$^{-/-}$ hyperproliferation. We stimulated purified naive CD4 T cells with PMA and ionomycin, which bypasses the TCR to induce activation and proliferation. Surprisingly, we found no change in proliferation between *Abcg1*$^{-/-}$ and B6 CD4 T cells, measured by CFSE dilution and ^{3}H-thymidine incorporation (Fig. 6E,6F). Therefore, we conclude that the mechanism by which ABCG1 regulates T cell proliferation is most likely through enhanced TCR signal strength.

Abcg1$^{-/-}$ T cells have increased TCR signaling

To determine whether the absence of ABCG1 in T cells alters TCR signaling, we stimulated B6 and *Abcg1*$^{-/-}$ naive CD4 T cells with αCD3 and αCD28 for short time periods and measured the phosphorylation of signaling proteins. Interestingly, we found an increase in the basal level of ZAP70 phosphorylation and a slight increase within 2 min after TCR stimulation in *Abcg1*$^{-/-}$ T cells (Fig. 7A). ZAP70 phosphorylation is a very early signaling event after TCR stimulation and branches to many signaling pathways (6). Next, we measured phospholipase C (PLCγ1) and found no difference in phosphorylation levels between B6 and *Abcg1*$^{-/-}$ T cells (Fig. 7A). We also observed no change in phosphorylation levels of p38, JNK1/2, or protein kinase C (Fig. 7A). However, we found a dramatic difference in the phosphorylation of ERK1/2. *Abcg1*$^{-/-}$ T cells seemed to have increased phosphorylated ERK1/2 levels under resting conditions; after stimulation, ERK1/2 phosphorylation levels were sustained longer than in B6 CD4 T cells (Fig. 7A). We think this is very interesting because the MAPK pathway is a major signal for cellular proliferation. To further support our hypothesis that *Abcg1*$^{-/-}$ T cells are hyperproliferative as the result of enhanced TCR signaling and ERK1/2 phosphorylation, we performed an in vitro proliferation assay in the presence of a MEK1/2 inhibitor, PD98059 (Fig. 7B). Strikingly, the inhibition of MEK1/2 completely reversed the hyperproliferative phenotype of *Abcg1*$^{-/-}$ naive CD4 T cells (Fig. 7B). There was no significant difference in thymidine incorporation between untreated B6 T cells and PD98059-treated *Abcg1*$^{-/-}$ T cells (Fig. 7B). This result provides further evidence that enhanced ERK1/2 phosphorylation causes hyperproliferation in *Abcg1*$^{-/-}$ CD4 T cells. We hypothesize that cholesterol accumulation in *Abcg1*$^{-/-}$ T cells affects the cell in many ways, and we found two specific mechanisms. First, increased cholesterol in the plasma membrane of *Abcg1*$^{-/-}$ T cells results in lipid raft formation and ZAP70 phosphorylation in resting, unstimulated T cells, making the *Abcg1*$^{-/-}$ T cells primed for stimulation. Second, the subcellular cholesterol distribution is affecting the basal and sustained phosphorylation of ERK1/2 in *Abcg1*$^{-/-}$ T cells. Clearly, cholesterol has the ability to modify the membrane and protein-signaling pathways.

Discussion

Understanding how cholesterol homeostasis impacts lymphocyte proliferation and function is very important, because proliferation is a key process in adapting an immune response to antigenic challenge. In the current study, we provide evidence that excess cellular cholesterol alters TCR signaling, resulting in hyperproliferation in developing and peripheral T cells. Our work is the first to describe a cell type in Abcg1-deficient mice with such a robust change in cholesterol content and expression of cholesterol metabolism genes (18, 27–29). This demonstrates the importance of ABCG1 expression in lymphocytes, particularly.

Cholesterol is a necessary component of membranes and is required for membrane formation during cell division. The ability of the T cell to regulate sterol levels during T cell activation is critical. Surprisingly, quantitative cholesterol levels are not often measured in lymphocytes. Bensinger et al. (12) recently provided evidence that T cell activation triggers the induction of sulfotransferase 2B1, an oxysterol-metabolizing enzyme, thus suppressing the LXR pathway for cholesterol transport and upregulating the SREBP pathway for cholesterol synthesis. *Lxrβ*-deficient mice exhibit a similar lymphocyte phenotype as *Abcg1*-deficient mice, with enhanced lymphocyte proliferation (12); however, $Lxr\beta^{-/-}$ mice have normal T cell development (12). Moreover, the cholesterol content in $Lxr\beta^{-/-}$ lymphocytes has not been described, nor has the mechanism by which $Lxr\beta^{-/-}$ lymphocytes are hyperproliferative. Our work provides insight into the understanding of sterol regulation in lymphocytes by quantitatively measuring cholesterol levels in CD4 T cells and describing a novel mechanism by which excess cholesterol results in enhanced signaling and hyperproliferation. Our results, combined with those of Bensinger et al. (12), begin to provide a complete story of lymphocyte function under high and low levels of sterol.

Our original hypothesis was that $Abcg1^{-/-}$ T cells are “primed” for proliferation as the result of increased cholesterol content. Once stimulated, the $Abcg1^{-/-}$ lymphocytes would progress more quickly through the cell cycle because they could satisfy the “cholesterol checkpoint” for cell division. However, when we stimulated $Abcg1^{-/-}$ T cells with PMA and ionomycin, we found no change in proliferation compared with B6 T cells (Fig. 6E,6F). If increased sterol availability alone can cause hyperproliferation, then T cell stimulation signals through the TCR should be irrelevant. Therefore, we examined how increased cholesterol content can affect TCR signaling. We went on to discover that $Abcg1^{-/-}$ T cells have enhanced phosphorylation of ZAP70 and ERK1/2 signaling proteins (Fig. 7A). Remarkably, the inhibition of MEK1/2, the upstream kinase of ERK1/2, completely reversed the hyperproliferative phenotype of $Abcg1^{-/-}$ naive CD4 T cells (Fig. 7B), demonstrating that enhanced downstream signaling of MEK1/2, possibly through ERK, causes hyperproliferation of $Abcg1^{-/-}$ T cells.

We were curious to determine whether enhanced TCR signaling in $Abcg1^{-/-}$ T cells resulted in increased IL-2 production. We measured higher levels of IL-2 protein in the supernatant of $Abcg1^{-/-}$ T cells after × d in culture, but after normalizing to total number of cells or cellular protein concentrations, there was no difference compared with B6 T cells (data not shown). We also measured the mRNA expression of IL-2 and found no difference between B6 and $Abcg1^{-/-}$ T cells. These data were surprising, but the ERK signaling pathway does not seem to be essential for IL-2 production (31–33). Therefore, our results reveal how cholesterol can fine-tune the ERK signaling pathway for proliferation.

The role of membrane cholesterol in T cell lipid rafts has been studied extensively. However, most of these studies use methyl-β-cyclodextrin to deplete membrane cholesterol levels, resulting in the disruption of lipid rafts and TCR signaling. Little work has been done

on how excess cellular cholesterol affects lipid raft formation and TCR signaling because of the difficulty in "cholesterol loading" cells. Two recent studies showed that cholesterol accumulation could alter lipid rafts and cell proliferation. Zhu et al. (34) demonstrated that *Abca1*$^{-/-}$ macrophages accumulated free cholesterol and had a significant increase in membrane lipid rafts. Wilhelm et al. (35) observed hyperproliferation and activation of T cells from *ldlr*$^{-/-}$*Apoa1*$^{-/-}$ mice fed an atherogenic diet and increased esterified cholesterol content in *ldlr*$^{-/-}$*Apoa1*$^{-/-}$ immune cells compared with *ldlr*$^{-/-}$ cells. We demonstrate that cholesterol-treated B6 T cells have a 30% increase in proliferation compared with untreated B6 T cells (Fig. 4D). The enhanced proliferation from cholesterol-loaded B6 T cells did not reach that of *Abcg1*$^{-/-}$ T cells (Fig. 4D). This may reflect the ability of cells under normal conditions to accumulate cholesterol. Cells are highly capable of maintaining cholesterol homeostasis and upregulate transporters to buffer excess cholesterol (30). Our study used *Abcg1*$^{-/-}$ T cells, which accumulate cholesterol without pharmacological treatment or forced cholesterol loading, to investigate how excess cholesterol can affect TCR signaling. We observed an increase in lipid rafts and basal phosphorylation levels of ZAP70 in resting *Abcg1*$^{-/-}$ T cells (Figs. 4C, 7A), suggesting *Abcg1*$^{-/-}$ T cells are "primed" for stimulation. This work has significant implications in human disease; according to the Centers for Disease Control and Prevention, 17% of adult Americans have high blood cholesterol (≥240 mg/dl total cholesterol). Whether high cholesterol results in cholesterol accumulation in T cells and how this affects the ability of the T cell to launch an immune response warrant further investigation.

We demonstrated a connection between enhanced TCR signaling and cholesterol homeostasis in *Abcg1*$^{-/-}$ naive CD4 T cells (Figs. 4A, 7A), but we also observed a disruption in cholesterol homeostasis in *Abcg1*$^{-/-}$ thymocytes (Fig. 4E). We hypothesize that TCR signaling in thymocytes is enhanced as well but do not have explicit evidence to support this. We do illustrate hyperproliferation of DN3 and DP thymocytes and an increase in the ratio of DN/DP thymocytes (Fig. 3C, 3D). Signals from the pre-TCR control proliferation in late DN3 thymocytes and during the DN–DP transition (5), but further experiments are needed to determine whether enhanced pre-TCR signals result in the hyperproliferation of *Abcg1*$^{-/-}$ thymocytes. Our results also revealed increased proliferation of *Abcg1*$^{-/-}$ DN2 thymocytes (Fig. 3C, 3D). At this stage, proliferation is dependent on c-kit and IL-7 signals (1, 2). Therefore, the absence of ABCG1 may affect the expression of cytokine receptors as well, by altering the ordering and structure of the plasma membrane. Membrane cholesterol depletion was also shown to result in the shedding of activation markers and cytokine receptors (36, 37). Perhaps the increase in membrane cholesterol in *Abcg1*$^{-/-}$ thymocytes can cause enhanced cytokine receptor signaling and proliferation of DN2 thymocytes. More work is needed to examine the effects of ABCG1 expression and cholesterol on signals for lymphocyte development.

Little is known about how cholesterol affects CD4/CD8-lineage commitment. *Abcg1*$^{-/-}$ mice had a similar frequency of CD4^{+} SP thymocytes, but we observed a 50% increase in the absolute number of CD4^{+} SP thymocytes (Fig. 2D, Table I). Furthermore, we observed a decrease in the frequency of CD8^{+} SP thymocytes, with no change in the number of CD8^{+} T cells (Fig. 2D, Table I). There are numerous models of CD4/CD8-lineage choice (38). Several models agree that short and/or weak TCR signals terminate *Cd4* transcription, whereas long and/or strong TCR signals terminate *Cd8* transcription. If these models are applied to *Abcg1*$^{-/-}$ mice, one would expect *Abcg1*$^{-/-}$ thymocytes with increased TCR signal strength and/or duration to terminate *Cd8* transcription, develop fewer CD8 SP T cells, and have increased CD4 SP T cells, which is exactly what we observed (Fig. 2D, Table I). Additionally, ERK signaling is required for CD4^{+} T cell lineage. Overexpression of a hypersensitive form of ERK2 will skew differentiation toward CD4 T cell commitment (31, 39). We observed amplified ERK signaling in *Abcg1*$^{-/-}$ peripheral CD4 T cells (Fig.

7A), which suggests that increased ERK signaling in *Abcg1*$^{-/-}$ thymocytes may be skewing the thymocytes to CD4 SP cells. The models of CD4/CD8-lineage choice are still highly debated; however, it is clear that TCR signaling is important, and cholesterol may play a role in regulating this process.

Our results demonstrate that ABCG1 is a negative regulator of peripheral CD4 T cell proliferation and TCR signaling. Deletion of negative regulators of TCR signaling, such as Cbl-b (40, 41), Itch (42), SHP-1 (43–45), PTEN (46), SIT (47) and others, results in T cell hyperreactivity and increased susceptibility to autoimmune diseases. The majority of these negative regulatory proteins support peripheral tolerance by raising the threshold of T cell activation to enforce the requirement for costimulation and limit activation by self-Ags. Studies are underway to determine whether *Abcg1*$^{-/-}$ mice are more susceptible to autoimmune diseases due to hyperproliferative T cells. Alternatively, *Abcg1*$^{-/-}$ mice may be protected from autoimmune diseases as the result of the elimination of T cells with high-affinity TCR during negative selection in the thymus. It will be interesting to determine whether ABCG1 expression affects the development of autoimmune disease. Additionally, using an LXR agonist to modulate ABCG1 expression and deplete cellular cholesterol may be a beneficial therapeutic in autoimmune diseases in which lymphocytes are hyperresponsive.

The role of ABCG1 in pulmonary disease and atherosclerosis has been studied extensively in our laboratory and by other investigators. The absence of ABCG1 in bone marrow–derived cells results in pulmonary lipidosis and massive inflammation (19, 20). Further studies will determine whether hyperproliferative *Abcg1*$^{-/-}$ T cells are contributing to this pulmonary disease. The atherosclerosis studies involving ABCG1 have been surprising and controversial (48–51). Our work sheds light on a fascinating concept: that the cholesterol-rich environment of the atherosclerotic lesion may influence the function of lymphocytes. If T lymphocytes in the lesion have ample cholesterol, TCR signaling could be enhanced, causing the T lymphocytes to proliferate more quickly and contribute to the inflammatory environment.

In summary, our work describes a novel mechanism by which increased cholesterol content can alter TCR signaling to result in hyperproliferation. Our results raise the possibility that dyslipidemia may alter lymphocyte function and cause hyperreactive T cells. Likewise, ABCG1 expression was shown to be down-regulated in macrophages isolated from mice and patients with type 2 diabetes (52, 53). Additional studies will investigate whether diabetes affects ABCG1 expression in lymphocytes, resulting in cholesterol accumulation and enhanced TCR signaling and proliferation. In conclusion, our results clearly demonstrate that ABCG1 expression is important in developing and peripheral T cells for regulating cholesterol homeostasis.

Supplementary Material

Refer to Web version on PubMed Central for supplementary material.

Acknowledgments

We thank Themis Karaoli, Marcus Skaflen, and Dr. Suseela Srinivasan (University of Virginia) for their guidance and help with experiments; Joanne Lannigan, Director of the University of Virginia Flow Cytometry Core Facility, for advice with flow cytometry analysis; and Dr. Margo Roberts (University of Virginia) for helpful discussions.

This work was supported by National Institutes of Health Grants P01HL55798 and R01 HL085790 (to C.C.H.), R01 HL094525 and P01 HL049373 (to J.S.P.), and the American Heart Association (to A.J.A).

Abbreviations used in this paper

ABCA1	ATP-binding cassette A1
ABCG1	ATP-binding cassette transporter G1
CT-B	cholera toxin B
DN	double negative
DP	double positive
HMG-CoA	3-hydroxy-3-methyl-glutaryl-CoA
LDLR	low-density lipoprotein receptor
LXR	liver X receptor
PLCγ1	phospholipase C
SP	single positive
SREBP	sterol regulatory element-binding protein

References

1. Cantrell DA. Transgenic analysis of thymocyte signal transduction. Nat. Rev. Immunol. 2002; 2:20–27. [PubMed: 11905834]
2. Rothenberg EV, Moore JE, Yui MA. Launching the T-cell-lineage developmental programme. Nat. Rev. Immunol. 2008; 8:9–21. [PubMed: 18097446]
3. Michie AM, Zúñiga-Pflücker JC. Regulation of thymocyte differentiation: pre-TCR signals and β-selection. Semin. Immunol. 2002; 14:311–323. [PubMed: 12220932]
4. Goldrath AW, Bevan MJ. Selecting and maintaining a diverse T-cell repertoire. Nature. 1999; 402:255–262. [PubMed: 10580495]
5. Freitas AA, Rocha B. Peripheral T cell survival. Curr. Opin. Immunol. 1999; 11:152–156. [PubMed: 10322146]
6. Abraham RT, Weiss A. Jurkat T cells and development of the T-cell receptor signalling paradigm. Nat. Rev. Immunol. 2004; 4:301–308. [PubMed: 15057788]
7. Kabouridis PS, Jury EC. Lipid rafts and T-lymphocyte function: implications for autoimmunity. FEBS Lett. 2008; 582:3711–3718. [PubMed: 18930053]
8. Jury EC, Flores-Borja F, Kabouridis PS. Lipid rafts in T cell signalling and disease. Semin. Cell Dev. Biol. 2007; 18:608–615. [PubMed: 17890113]
9. Ikonen E. Cellular cholesterol trafficking and compartmentalization. Nat. Rev. Mol. Cell Biol. 2008; 9:125–138. [PubMed: 18216769]
10. Brown MS, Goldstein JL. Cholesterol feedback: from Schoenheimer's bottle to Scap's MELADL. J. Lipid Res. 2009; 50(Suppl):S15–S27. [PubMed: 18974038]
11. Tontonoz P, Mangelsdorf DJ. Liver X receptor signaling pathways in cardiovascular disease. Mol. Endocrinol. 2003; 17:985–993. [PubMed: 12690094]
12. Bensinger SJ, Bradley MN, Joseph SB, Zelcer N, Janssen EM, Hausner MA, Shih R, Parks JS, Edwards PA, Jamieson BD, et al. LXR signaling couples sterol metabolism to proliferation in the acquired immune response. Cell. 2008; 134:97–111. [PubMed: 18614014]
13. Wang N, Ranalletta M, Matsuura F, Peng F, Tall AR. LXR-induced redistribution of ABCG1 to plasma membrane in macrophages enhances cholesterol mass efflux to HDL. Arterioscler. Thromb. Vasc. Biol. 2006; 26:1310–1316. [PubMed: 16556852]
14. Xie Q, Engel T, Schnoor M, Niehaus J, Hofnagel O, Buers I, Cullen P, Seedorf U, Assmann G, Lorkowski S. Cell surface localization of ABCG1 does not require LXR activation. Arterioscler. Thrombosis. Vasc. Biol. 2006; 26:e143–144.

15. Tarr PT, Edwards PA. ABCG1 and ABCG4 are coexpressed in neurons and astrocytes of the CNS and regulate cholesterol homeostasis through SREBP-2. J. Lipid Res. 2008; 49:169–182. [PubMed: 17916878]

16. Savary S, Denizot F, Luciani M, Mattei M, Chimini G. Molecular cloning of a mammalian ABC transporter homologous to Drosophila white gene. Mamm. Genome. 1996; 7:673–676. [PubMed: 8703120]

17. Croop JM, Tiller GE, Fletcher JA, Lux ML, Raab E, Goldenson D, Son D, Arciniegas S, Wu RL. Isolation and characterization of a mammalian homolog of the Drosophila white gene. Gene. 1997; 185:77–85. [PubMed: 9034316]

18. Kennedy MA, Barrera GC, Nakamura K, Baldán A, Tarr P, Fishbein MC, Frank J, Francone OL, Edwards PA. ABCG1 has a critical role in mediating cholesterol efflux to HDL and preventing cellular lipid accumulation. Cell Metab. 2005; 1:121–131. [PubMed: 16054053]

19. Baldán A, Tarr P, Vales CS, Frank J, Shimotake TK, Hawgood S, Edwards PA. Deletion of the transmembrane transporter ABCG1 results in progressive pulmonary lipidosis. J. Biol. Chem. 2006; 281:29401–29410. [PubMed: 16887795]

20. Wojcik AJ, Skaflen MD, Srinivasan S, Hedrick CC. A critical role for ABCG1 in macrophage inflammation and lung homeostasis. J. Immunol. 2008; 180:4273–4282. [PubMed: 18322240]

21. Baldán A, Gomes AV, Ping P, Edwards PA. Loss of ABCG1 results in chronic pulmonary inflammation. J. Immunol. 2008; 180:3560–3568. [PubMed: 18292583]

22. Attie AD. ABCA1: at the nexus of cholesterol, HDL and atherosclerosis. Trends Biochem. Sci. 2007; 32:172–179. [PubMed: 17324574]

23. Maxfield FR, Tabas I. Role of cholesterol and lipid organization in disease. Nature. 2005; 438:612–621. [PubMed: 16319881]

24. Rudel LL, Kelley K, Sawyer JK, Shah R, Wilson MD. Dietary monounsaturated fatty acids promote aortic atherosclerosis in LDL receptor-null, human ApoB100-overexpressing transgenic mice. Arterioscler. Thromb. Vasc. Biol. 1998; 18:1818–1827. [PubMed: 9812923]

25. Livak KJ, Schmittgen TD. Analysis of relative gene expression data using real-time quantitative PCR and the 2(-Delta Delta C(T)) Method. Methods. 2001; 25:402–408. [PubMed: 11846609]

26. Kabouridis PS, Janzen J, Magee AL, Ley SC. Cholesterol depletion disrupts lipid rafts and modulates the activity of multiple signaling pathways in T lymphocytes. Eur. J. Immunol. 2000; 30:954–963. [PubMed: 10741414]

27. Yvan-Charvet L, Ranalletta M, Wang N, Han S, Terasaka N, Li R, Welch C, Tall AR. Combined deficiency of ABCA1 and ABCG1 promotes foam cell accumulation and accelerates atherosclerosis in mice. J Clin Invest. 2007; 117:3900–3908. [PubMed: 17992262]

28. Wang N, Yvan-Charvet L, Lütjohann D, Mulder M, Vanmierlo T, Kim TW, Tall AR. ATP-binding cassette transporters G1 and G4 mediate cholesterol and desmosterol efflux to HDL and regulate sterol accumulation in the brain. FASEB J. 2008; 22:1073–1082. [PubMed: 18039927]

29. Terasaka N, Yu S, Yvan-Charvet L, Wang N, Mzhavia N, Langlois R, Pagler T, Li R, Welch CL, Goldberg IJ, et al. ABCG1 and HDL protect against endothelial dysfunction in mice fed a high-cholesterol diet. J. Clin. Invest. 2008; 118:3701–3713. [PubMed: 18924609]

30. Radhakrishnan A, Goldstein JL, McDonald JG, Brown MS. Switch-like control of SREBP-2 transport triggered by small changes in ER cholesterol: a delicate balance. Cell Metab. 2008; 8:512–521. [PubMed: 19041766]

31. Rincón M. MAP-kinase signaling pathways in T cells. Curr. Opin. Immunol. 2001; 13:339–345. [PubMed: 11406366]

32. Rincón M, Flavell RA, Davis RJ. Signal transduction by MAP kinases in T lymphocytes. Oncogene. 2001; 20:2490–2497. [PubMed: 11402343]

33. Alberola-Ila J, Hogquist KA, Swan KA, Bevan MJ, Perlmutter RM. Positive and negative selection invoke distinct signaling pathways. J. Exp. Med. 1996; 184:9–18. [PubMed: 8691153]

34. Zhu X, Lee JY, Timmins JM, Brown JM, Boudyguina E, Mulya A, Gebre AK, Willingham MC, Hiltbold EM, Mishra N, et al. Increased cellular free cholesterol in macrophage-specific Abca1 knock-out mice enhances pro-inflammatory response of macrophages. J. Biol. Chem. 2008; 283:22930–22941. [PubMed: 18552351]

35. Wilhelm AJ, Zabalawi M, Grayson JM, Weant AE, Major AS, Owen J, Bharadwaj M, Walzem R, Chan L, Oka K, et al. Apolipoprotein A-I and its role in lymphocyte cholesterol homeostasis and autoimmunity. Arterioscler. Thromb. Vasc. Biol. 2009; 29:843–849. [PubMed: 19286630]
36. von Tresckow B, Kallen KJ, von Strandmann EP, Borchmann P, Lange H, Engert A, Hansen HP. Depletion of cellular cholesterol and lipid rafts increases shedding of CD30. J. Immunol. 2004; 172:4324–4331. [PubMed: 15034047]
37. Matthews V, Schuster B, Schütze S, Bussmeyer I, Ludwig A, Hundhausen C, Sadowski T, Saftig P, Hartmann D, Kallen KJ, et al. Cellular cholesterol depletion triggers shedding of the human interleukin-6 receptor by ADAM10 and ADAM17 (TACE). J. Biol. Chem. 2003; 278:38829–38839. [PubMed: 12832423]
38. Singer A, Adoro S, Park JH. Lineage fate and intense debate: myths, models and mechanisms of CD4- versus CD8-lineage choice. Nat. Rev. Immunol. 2008; 8:788–801. [PubMed: 18802443]
39. Sharp LL, Schwarz DA, Bott CM, Marshall CJ, Hedrick SM. The influence of the MAPK pathway on T cell lineage commitment. Immunity. 1997; 7:609–618. [PubMed: 9390685]
40. Krawczyk C, Bachmaier K, Sasaki T, Jones RG, Snapper SB, Bouchard D, Kozieradzki I, Ohashi PS, Alt FW, Penninger JM. Cbl-b is a negative regulator of receptor clustering and raft aggregation in T cells. Immunity. 2000; 13:463–473. [PubMed: 11070165]
41. Bachmaier K, Krawczyk C, Kozieradzki I, Kong YY, Sasaki T, Oliveira-dos-Santos A, Mariathasan S, Bouchard D, Wakeham A, Itie A, et al. Negative regulation of lymphocyte activation and autoimmunity by the molecular adaptor Cbl-b. Nature. 2000; 403:211–216. [PubMed: 10646608]
42. Fang D, Elly C, Gao B, Fang N, Altman Y, Joazeiro C, Hunter T, Copeland N, Jenkins N, Liu YC. Dysregulation of T lymphocyte function in itchy mice: a role for Itch in TH2 differentiation. Nat. Immunol. 2002; 3:281–287. [PubMed: 11828324]
43. Lorenz U, Ravichandran KS, Burakoff SJ, Neel BG. Lack of SHPTP1 results in src-family kinase hyperactivation and thymocyte hyper-responsiveness. Proc. Natl. Acad. Sci. USA. 1996; 93:9624–9629. [PubMed: 8790380]
44. Pani G, Fischer KD, Mlinaric-Rascan I, Siminovitch KA. Signaling capacity of the T cell antigen receptor is negatively regulated by the PTP1C tyrosine phosphatase. J. Exp. Med. 1996; 184:839–852. [PubMed: 9064344]
45. Kon-Kozlowski M, Pani G, Pawson T, Siminovitch KA. The tyrosine phosphatase PTP1C associates with Vav, Grb2, and mSos1 in hematopoietic cells. J. Biol. Chem. 1996; 271:3856–3862. [PubMed: 8632004]
46. Suzuki A, Yamaguchi MT, Ohteki T, Sasaki T, Kaisho T, Kimura Y, Yoshida R, Wakeham A, Higuchi T, Fukumoto M, et al. T cell-specific loss of Pten leads to defects in central and peripheral tolerance. Immunity. 2001; 14:523–534. [PubMed: 11371355]
47. Simeoni L, Posevitz V, Kölsch U, Meinert I, Bruyns E, Pfeffer K, Reinhold D, Schraven B. The transmembrane adapter protein SIT regulates thymic development and peripheral T-cell functions. Mol. Cell. Biol. 2005; 25:7557–7568. [PubMed: 16107703]
48. Baldán A, Pei L, Lee R, Tarr P, Tangirala RK, Weinstein MM, Frank J, Li AC, Tontonoz P, Edwards PA. Impaired development of atherosclerosis in hyperlipidemic Ldlr$^{-/-}$ and ApoE$^{-/-}$ mice transplanted with Abcg1$^{-/-}$ bone marrow. Arterioscler. Thromb. Vasc. Biol. 2006; 26:2301–2307. [PubMed: 16888235]
49. Ranalletta M, Wang N, Han S, Yvan-Charvet L, Welch C, Tall AR. Decreased atherosclerosis in low-density lipoprotein receptor knockout mice transplanted with Abcg1$^{-/-}$ bone marrow. Arterioscler. Thromb. Vasc. Biol. 2006; 26:2308–2315. [PubMed: 16917103]
50. Out R, Hoekstra M, Hildebrand RB, Kruit JK, Meurs I, Li Z, Kuipers F, Van Berkel TJ, Van Eck M. Macrophage ABCG1 deletion disrupts lipid homeostasis in alveolar macrophages and moderately influences atherosclerotic lesion development in LDL receptor-deficient mice. Arterioscler. Thromb. Vasc. Biol. 2006; 26:2295–2300. [PubMed: 16857950]
51. Out R, Hoekstra M, Meurs I, de Vos P, Kuiper J, Van Eck M, Van Berkel TJ. Total body ABCG1 expression protects against early atherosclerotic lesion development in mice. Arterioscler. Thromb. Vasc. Biol. 2007; 27:594–599. [PubMed: 17204665]

52. Mauldin JP, Srinivasan S, Mulya A, Gebre A, Parks JS, Daugherty A, Hedrick CC. Reduction in ABCG1 in type 2 diabetic mice increases macrophage foam cell formation. J. Biol. Chem. 2006; 281:21216–21224. [PubMed: 16723355]

53. Mauldin JP, Nagelin MH, Wojcik AJ, Srinivasan S, Skaflen MD, Ayers CR, McNamara CA, Hedrick CC. Reduced expression of ATP-binding cassette transporter G1 increases cholesterol accumulation in macrophages of patients with type 2 diabetes mellitus. Circulation. 2008; 117:2785–2792. [PubMed: 18490524]

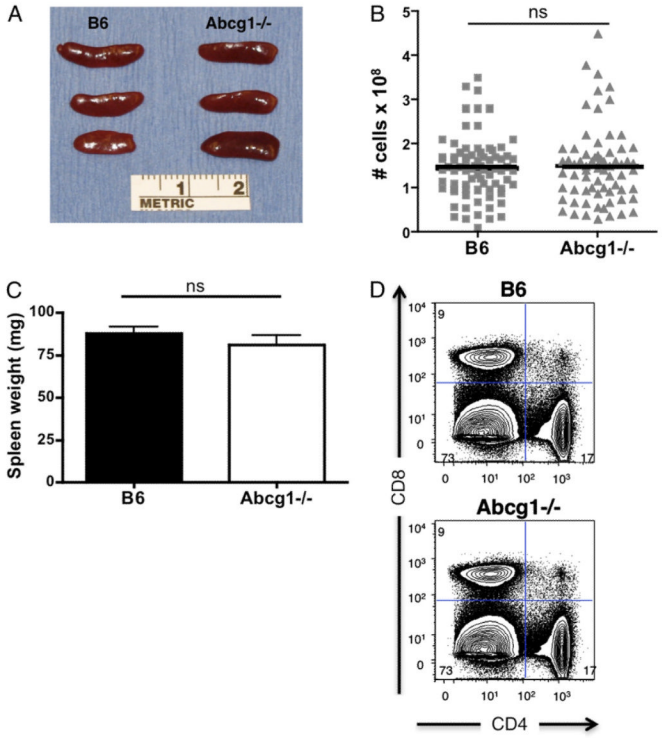

FIGURE 1.

Abcg1$^{-/-}$ spleen and CD4/CD8 frequencies appear normal. *A*, Gross morphology of spleens from 6- to 8-wk-old mice. *B*, Graph of total spleen cellularity. *C*, Graph of spleen weight. *D*, Representative plots of frequency of CD4^{+} and CD8^{+} lymphocytes.

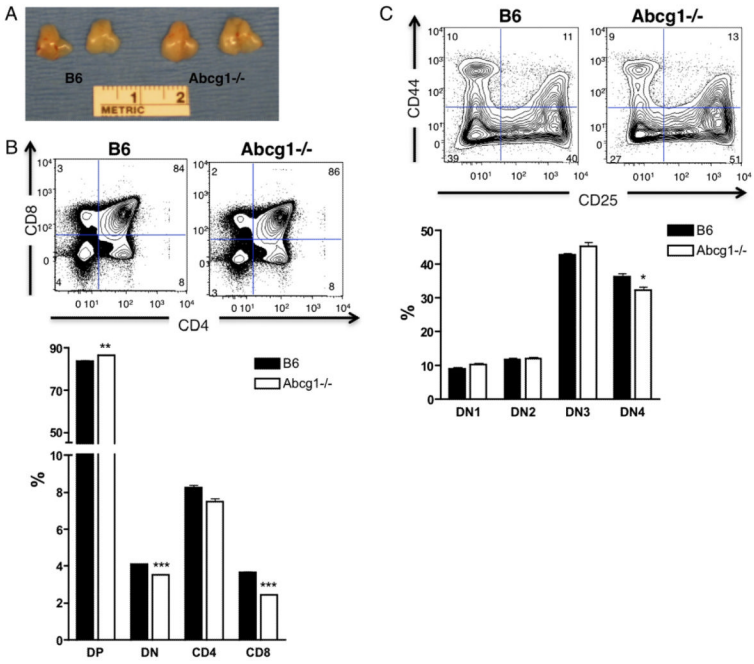

FIGURE 2.

ABCG1 regulates thymocyte development. *A*, Gross morphology of thymus from 5-wk-old mice. *B*, Representative plots of frequency of $CD4^+CD8^+$ (DP), $CD4^-CD8^-$ (DN), $CD4^+CD8^-$ (CD4 SP), and $CD4^-CD8^+$ (CD8 SP) thymocytes and graph representation (n = 13). *C*, Representative plots of frequency of CD25 versus CD44 populations on lineage (CD4, CD8, CD3, CD19, Mac1, Gr1, Ter119, NK1.1)-negative DN thymocytes and graph representation (n = 12). *p < 0.05; **p < 0.01; ***p < 0.0001.

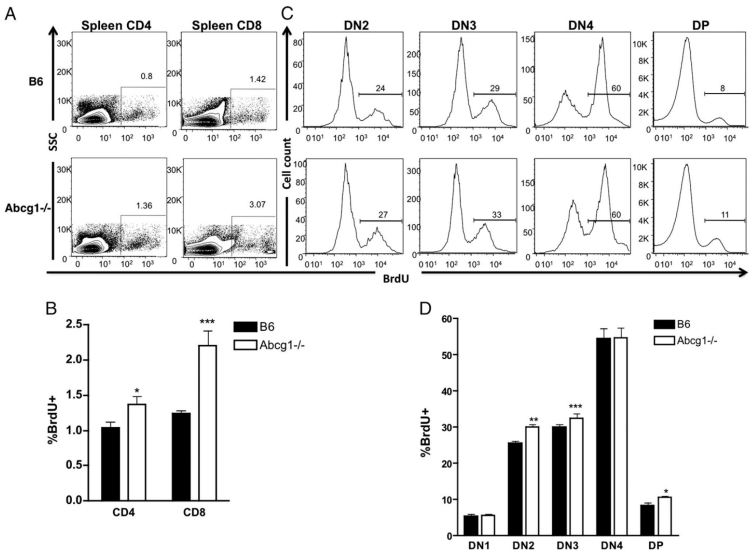

FIGURE 3.

Abcg1$^{-/-}$ mice have increased thymocyte and peripheral lymphocyte proliferation in vivo. Five-week-old B6 (n = 8) and *Abcg1*$^{-/-}$ (n = 8) mice were injected with 1 mg of BrdU and sacrificed 4 h later. *A*, Representative plots SSC versus BrdU of CD4^{+}CD3^{+} T cells and CD8^{+}CD3^{+} T cells from the spleen. *B*, Graph of frequencies of CD4^{+} or CD8^{+} T cells that incorporated BrdU. *C*, Representative histograms of BrdU+ cells in lineage (CD4, CD8, CD3, CD19, Mac1, Gr1, Ter119, NK1.1)-negative DN thymocyte subsets DN2 (CD25+CD44+), DN3 (CD25+CD44−) DN4 (CD25−CD44−), and DP (CD4+CD8+) thymocytes and (*D*) graph of frequencies of cells in each thymocyte subset that incorporated BrdU. *p < 0.05; **p < 0.01; ***p < 0.0001.

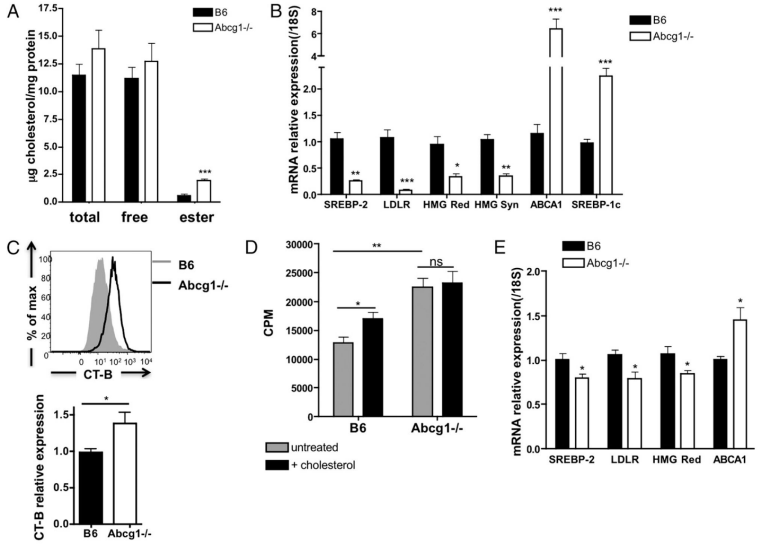

FIGURE 4.

Abcg1$^{-/-}$ CD4 T cells have increased cholesterol content. *A*, Total cholesterol and free cholesterol was measured in purified CD4 T cells by gas chromatography ($n = 7$). Cholesteryl ester was calculated as the difference between total and free cholesterol (multiplied by 1.67). *B*, SREBP-2 and LXR targets genes measured in naive CD4 T cells by real-time PCR ($n = 6$–10). *C*, Lipid rafts were measured in CD4 T cells by flow cytometry using fluorescently labeled CT-B (see *Materials and Methods*). A representative intensity plot of B6 and *Abcg1*$^{-/-}$ lipid raft staining. Graph represents relative expression to B6 mean fluorescence intensity of CT-B Alexa Fluor 488 ($n = 15$). *D*, Naive CD4 T cells were purified from B6 and *Abcg1*$^{-/-}$ mice ($n = 4$), incubated with 20 μg/ml soluble cholesterol for 2 h, and stimulated with αCD3αCD28 beads. ^{3}H thymidine was added to cultures after a 48-h stimulation and harvested after 18 h. *E*, SREBP-2 and LXR target genes measured in thymocytes by real-time PCR ($n = 6$–10). *$p < 0.05$; **$p < 0.01$; ***$p < 0.001$.

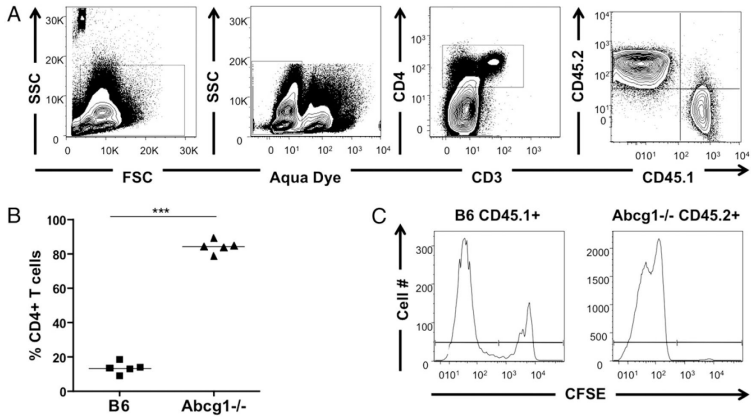

FIGURE 5.

Abcg1$^{-/-}$ CD4 T cells have a homeostatic proliferative advantage. B6 (CD45.1^{+}) and *Abcg1*$^{-/-}$ (CD45.2^{+}) naive CD4 T cells were purified from spleen, labeled with CFSE, and coinjected into *RAG*$^{-/-}$ mice. After 7 d, the spleen was harvested and stained for proliferating T cells. *A*, Cells were gated on forward light scatter versus SSC, aqua LIVE/DEAD negative, CD4^{+}, and CD45.1^{+} or CD45.2^{+}. *B*, Percentage of CD4 T cells that are B6 or *Abcg1*$^{-/-}$. $n = 5$, repeated twice. ***$p < 0.0001$. *C*, CFSE dilution of CD45.1^{+} or CD45.2^{+} CD4 T cells.

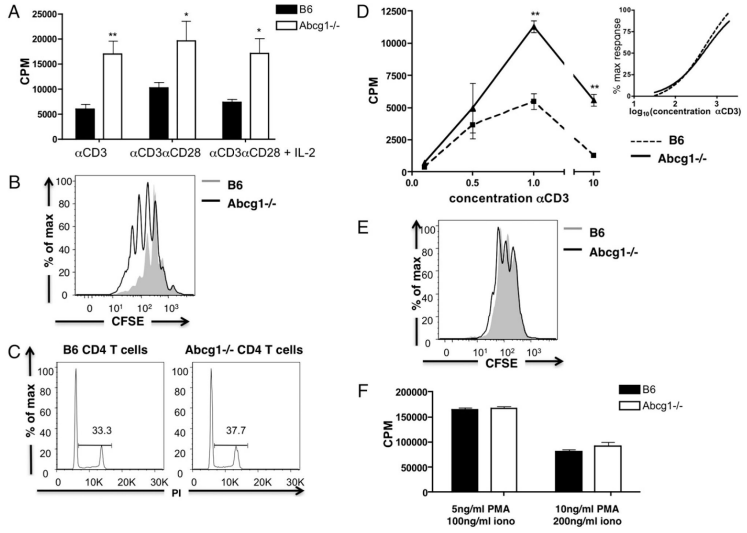

FIGURE 6.

Naive CD4 T cells from *Abcg1*$^{-/-}$ mice are hyperproliferative to TCR stimulation. Naive CD4 T cells were purified from spleen. *A*, Cells (n = 4) were stimulated with plate-bound αCD3 (1 μg/ml), soluble αCD28 (1 μg/ml), and IL-2 (10 U/ml). ^{3}H thymidine was added to cultures after a 48-h stimulation and harvested after 18 h. *B*, CFSE-labeled cells (n = 4) were stimulated with 1 μg/ml plate-bound αCD3 and 1 μg/ml αCD28, and CFSE dilution was measured after 72 h. *C*, Cells (n = 3) were stimulated with 1 μg/ml plate-bound αCD3 and 1 μg/ml αCD28 and stained with propidium iodide after 48 h to determine the cell cycle. *D*, Cells (n = 4) were stimulated with 0.1–10 μg/ml plate-bound αCD3 and 1 μg/ml soluble αCD28, and ^{3}H thymidine incorporation was measured. Graph represents ^{3}H thymidine incorporation (inset). Nonlinear curve regression was used to fit the data to sigmoidal curves and calculate EC_{50}. *E*, CFSE-labeled cells (n = 6) were stimulated with 5 ng/ml PMA and 100 ng/ml ionomycin, and CFSE dilution was measured after 72 h. *F*, Cells (n = 4) were stimulated with PMA and ionomycin (iono), and ^{3}H thymidine incorporation was measured. *$p < 0.05$; **$p < 0.01$; ***$p < 0.0001$.

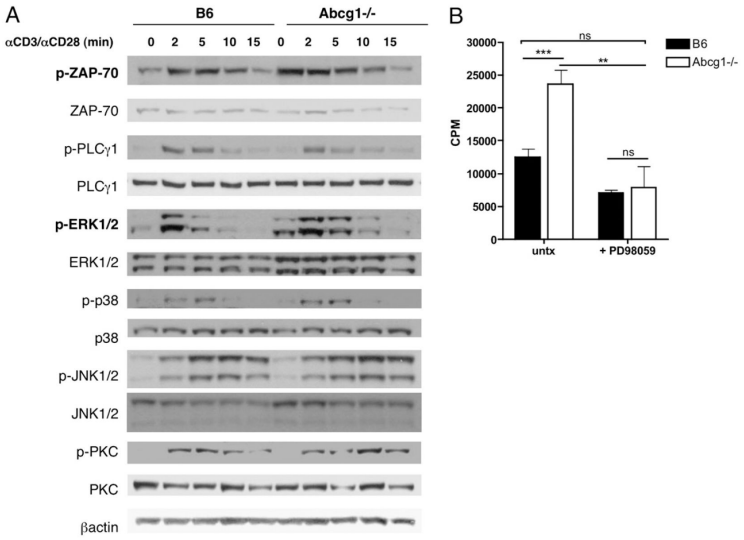

FIGURE 7.

Enhanced ERK1/2 phosphorylation results in hyperproliferation of *Abcg1*$^{-/-}$ CD4 T cells. *A*, B6 and *Abcg1*$^{-/-}$ naive CD4 T cells were stimulated with cross-linked anti-CD3 and anti-CD28 mAbs for the indicated times. Cell lysates were separated by SDS-PAGE and immunoblotted with the indicated Abs. Each blot was repeated twice. *B*, B6 and *Abcg1*$^{-/-}$ naive CD4 T cells ($n = 4$) were stimulated with plate-bound αCD3 (1 μg/ml) and soluble αCD28 (1 μg/ml) in the presence or absence (untx) of 10 μM PD98059. ^{3}H thymidine was added to cultures after a 48-h stimulation and harvested after 18 h. $^{**}p < 0.01$; $^{***}p < 0.001$.

Table I

Comparison of absolute cell numbers among the thymocyte subsets

Phenotype	Total	DP	DN	CD4 SP	CD8 SP
B6	$215 \times 10^6 \pm 7$	$172 \times 10^6 \pm 5$	$8.4 \times 10^6 \pm 0.2$	$17.0 \times 10^6 \pm 1.0$	$7.5 \times 10^6 \pm 0.4$
Abcg1 $^{-/-}$	$346 \times 10^6 \pm 14^*$	$267 \times 10^6 \pm 1^*$	$11.9 \times 10^6 \pm 0.5^*$	$26.0 \times 10^6 \pm 2.4^\dagger$	$8.3 \times 10^6 \pm 0.6$

Total cell numbers were determined by multiplying the frequency of each subset (measured by flow cytometry) by the total cell count (measured by microscopic counting) (n = 13).

$^*p < 0.0001$;

$^\dagger p < 0.001$.